Meteorol. Z. (Contrib. Atm. Sci.)
Published online September 2026

Open Access
Early Access MetTools

CC BY

Hunting and harvesting urban climate data through mobile measurements with different platforms across various local climate zones

Uta Moderow[1,*], Astrid Ziemann[1], Valeri Goldberg[1], Peter Dietrich[2], Uta Ködel[2], Claudia Schütze[2,3]

[1] Technische Universität Dresden, Faculty of Environmental Sciences, Department of Hydrosciences, Chair of Meteorology, Dresden, Germany
[2] Helmholtz Centre for Environmental Research GmbH – UFZ, Department Monitoring and Exploration Technologies, Leipzig, Germany
[3] Umweltbundesamt (UBA) – German Environment Agency, Wörlitzer Platz 1, 06844 Dessau-Roßlau, Germany
* Corresponding author: uta.moderow@tu-dresden.de

With 12 figures, 9 tables and 8 appendices

Abstract: In a joint effort of two projects (Urban Forest and CityCLIM), mobile micrometeorological measurements were carried out in the city of Leipzig in Central Germany. Three different platforms (bike, car, and pedestrian with backpack) were used alongside three stationary measurement stations. The measurement equipment included low-cost sensors designed specifically for citizen science contexts, such as the MeteoTracker and SenseBox as well as equipment typically used in professional settings. Citizen volunteers were involved in the data collection as part of the EU Horizon 2020 CityCLIM project. These measurements provided the opportunity to address various aspects of urban climate-related research. This paper focuses on three key aspects. First, we analyze the impact of radiation errors on the quality of mobile air temperature measurements and their potential effect on accurately capturing air temperature trends. Secondly, we examine the similarities and differences in measurement results between citizen science (CS) instruments and those of professional standards with the primary goal of refining the basis for appropriate guidelines for CS measurements. Thirdly, we address the question of whether air temperature measurements by CS systems would be sufficient for assessing heat stress. Our results show that CS devices can capture the daily variation in air temperature but exhibit larger radiation errors during periods of high incoming radiation and insufficient ventilation. The results also indicate that air temperature measurements do not always accurately identify areas with high potential of heat stress. Furthermore, the spatial variability of air temperature is significantly lower than that of heat stress, whereas the highest variability was found for surface temperature of the ground.

Keywords: urban climate; mobile measurements; citizen science; local climate zones; UTCI

1 Introduction

Cities are typically warmer than rural areas due to the urban heat island effect (UHI). This phenomenon raises concerns for public health, energy and urban management (Johnson & Wilson 2009; Ohashi et al. 2007; Tong et al. 2021) in relation to negative effects of heat stress within cities. However, experienced heat stress depends more strongly on the local microclimate variability within a city than on the area-averaged or larger-scale UHI effect.

A common method to assess urban climate variability is the local climate zone (LCZ) framework (Stewart & Oke 2012). It classifies urban and rural areas based on land cover, urban structure, and surface characteristics. This allows the identification of climate-relevant intra-urban differences, such as variations in vegetation, surface materials, and the degree of imperviousness. However, notable differences can also occur within the same LCZ due to changes in vegetation cover, building density, and surface properties. These local variations can strongly affect the microclimate and should be considered in urban climate studies (Oke et al. 2017).

Urban climate variability can be assessed by models or measurements, including ground-based and remote sensing methods. This study focuses on ground-based measurements. Urban areas are highly structured and show strong spatial variability in meteorological conditions, making measurements challenging. A single stationary climate station is only representative of similar surroundings, while the

DOI: 10.1127/metz/1277
© 2026 The authors
Gebrüder Borntraeger Science Publishers, Stuttgart, www.borntraeger-cramer.com

expansion of monitoring networks is often constrained by administrative regulations, site availability, costs, and maintenance requirements. Vandalism is an additional challenge in urban environments.

Mobile measurements help to address spatial gaps in urban meteorological observations by covering larger areas and locations that are not monitored by stationary stations. They capture spatial variability in meteorological conditions relevant to human heat exposure, which would otherwise require a very dense fixed network. Human bioclimatic indices derived from these data estimate heat stress for a person remaining at a given location for a sufficient period, although physiological responses are not measured. Mobile measurements can be conducted using bicycles (Heusinkveld et al. 2014; Samad & Vogt 2020; Yokoyama et al. 2018), cars (Gracia-León et al. 2021; Junk et al. 2003; Leconte et al. 2020), public transportation such as buses or trams (Hagemann et al. 2014; Hoffmann & Kreienkamp 2019; Todorov et al. 2023) or backpack systems (Gallinelli et al. 2017; Moderow et al. 2023; Tsin et al. 2016), and more recently with low-cost sensors in CS projects (Demuth et al. 2013; Loglisci et al. 2024). This approach allows the collection of large datasets, fosters public participation, and supports environmental modelling (Hooyberghs et al. 2022; Nipen et al. 2020). However, guidelines for CS data collection are often lacking, although they are essential to ensure data quality (Beck & Mitkiewicz 2025; Middel et al. 2022; Schmidt et al. 2023).

The study combines mobile measurements and CS to evaluate different mobile systems, assess the suitability of air temperature for estimating pedestrian heat stress, and develop recommendations for CS guidelines. It addresses the following research questions:

(1) What is the influence of radiation errors on the performance of mobile systems for measuring the diurnal cycle of air temperature?
(2) To what extent can air temperature be used to assess heat stress of pedestrians compared to other thermal variables or thermal indices?
(3) What recommendations can be derived for CS measurements that rely solely on air temperature to assess heat stress?

These questions are examined based on a measurement campaign conducted in Leipzig over approximately two summer days using three different mobile systems (car, bicycle, backpack) alongside stationary reference measurements.

2 Material and methods

2.1 Site description

Measurements were conducted in Leipzig, a city in the southeastern Germany. The core project area is located in the Plagwitz district, adjacent to a former railway freight yard. After industrial decline in the 1990s, the area was partly afforested in 2015 as part of the "Urbane Wälder" project (Rink & Schmidt 2021), while other sections, especially the area south of Antonienbrücke (Fig. 1), were left to natural succession.

The surrounding neighbourhood is characterised by dense 19th-century development with narrow streets and limited green space, with industrial and commercial uses mainly north of Antonienstraße and residential areas to the south (Fig. 1).

Local Climate Zones (LCZ; Stewart & Oke 2012, Fig. 1c) were used to describe the urban structure. LCZ units typically cover 200–500 m and often extend over 0.5–2 km². WUDAPT LCZ data, based on Landsat imagery with 30 m resolution and mapped on 100 x 100 m² grid, represent building conditions from 2016. LCZs (Demuzere et al. 2019, 2020) were obtained from the WUDAPT database (https://www.wudapt.org/lcz-maps/, accessed 12. February 2024) and are shown in Fig. 1c. This dataset is representative of the building status in 2016. As no relevant structural changes has occurred in the area since 2016, the LCZ classification is considered valid for 2023.

2.2 Meteorological conditions

During the measurement campaign, weather conditions were dominated by a high-pressure system extending from the Bay of Biscay to Poland. This anti-cyclonic situation caused fair weather with mainly light northerly to north-easterly winds. Moist air from the Alpine region led to high vapour pressure and, together with high air temperatures, resulted in heat-stress conditions suitable for the measurement campaign.

Local meteorological conditions are shown in Fig. 2 using data from the Leipzig-Holzhausen and Leipzig/Halle Airport stations, both operated by the German Meteorological Service (DWD) and compliant with WMO standards. Leipzig-Holzhausen is located about 9 km from the study area and represents suburban conditions (Behrens & Hoffmann 2016), while Leipzig/Halle Airport station is about 14 km to the north (Fig. 1a).

2.3 Mobile measurement systems

Three different mobile systems were employed: a backpack-based carrier device developed at TU Dresden (Moderow et al. 2023), the MeteoTracker (Loglisci et al. 2024), and the SenseBox (Demuth et al. 2013). The latter two devices are typically used in CS projects, whereas the TU Dresden backpack system is designed to meet the standards of professional research.

2.3.1 Mobile systems using bicycles and cars as carrier system

The SenseBox (Reedu GmbH & Co. KG, Germany; Fig. 3) is a toolkit for environmental monitoring especially designed for flexible use in CS projects. Its primarily designed for educational purposes, emphasizing the learning benefits of personal assembly and programming. Due to the modular concept, various sensors are available to monitor physical and chemical properties of the atmosphere and the soil. The SenseBox sys-

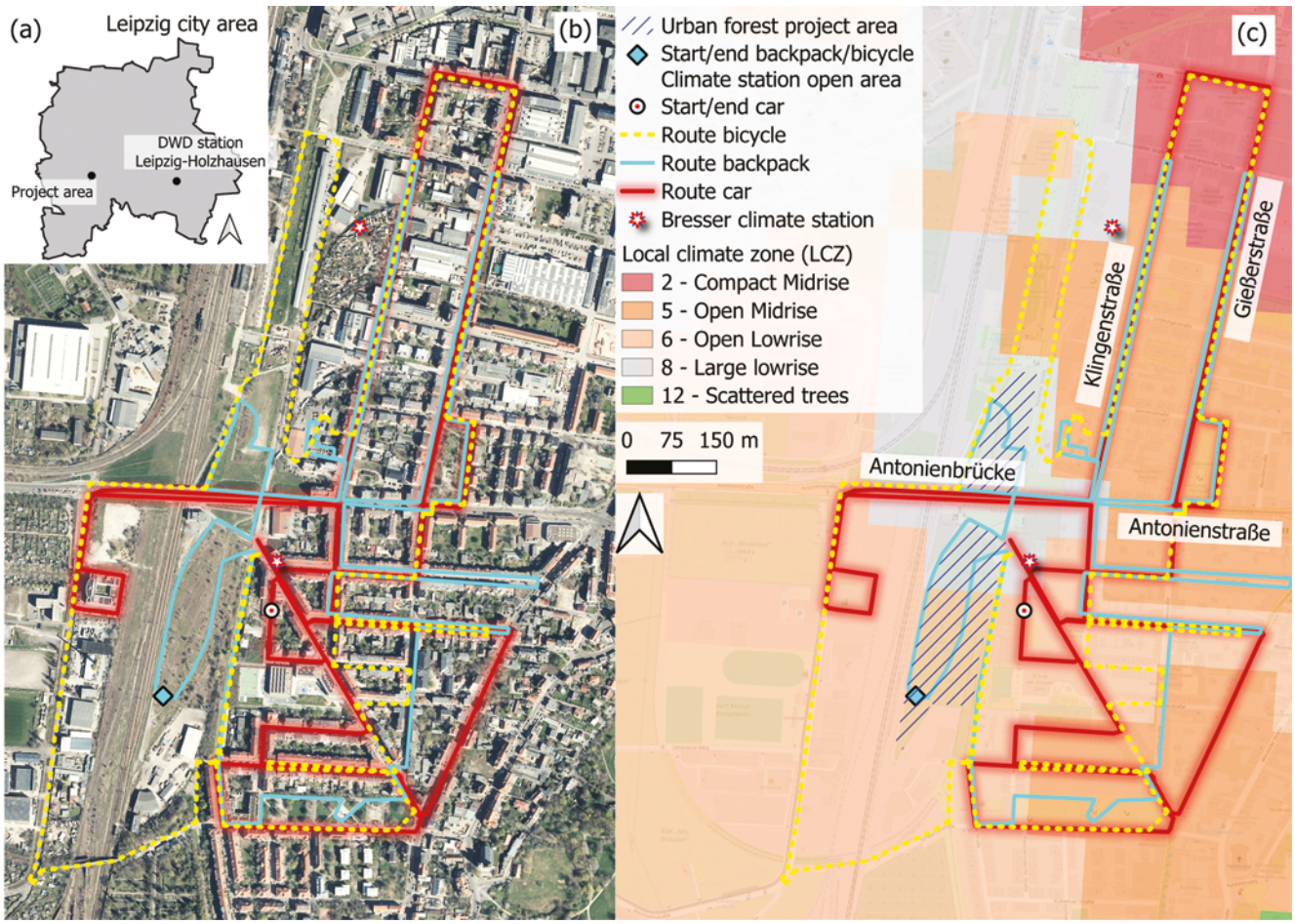

Fig. 1. (a) City area of Leipzig (gray). The locations of the project area and the German Meteorological Service (DWD) station Leipzig-Holzhausen are shown. (b) Overview of the investigated area and tracks of the different mobile platforms. (c) Open Street map overlaid with local climate zones. The hatched area denotes the core project area of the urban forest, with natural succession in the southern part and reforestation with limited success in the northern part (see Fig. 1b). Scale and north arrow refer to maps (b) and (c). Orthophoto: Open Geodata Freestate of Saxony, Germany, Datenlizenz Deutschland – Zero – Version 2.0, https://www.govdata.de/dl-de/zero-2-0. Open Street Map: OpenStreetMap contributors. (2025). Map data retrieved from OpenStreetMap via QGIS (version 3.40). Retrieved 02.09.2025, from https://www.openstreetmap.org.

tem is based on an easy-to-program Arduino microcontroller unit and can be connected via WiFi or LoRaWAN to a web-based dashboard platform that provides the data online in real time. A large and active community continuously develops the platform and supports its users. The deployed SenseBox system consists of a multi-parameter sensor for air temperature, air humidity, and air pressure, a CO_2 concentration sensor, a GPS sensor, and a dust sensor measuring particle concentrations between 0.3 to 10 µm in the air.

The MeteoTracker (IOTOPON SRL, Italy; Fig. 4) is a mobile system for real-time weather data collection and analysis. It consists of a compact sensor that can be mounted on vehicles or other mobile platforms, such as bicycles, and a smartphone app that collects, visualises, and analyses the data. MeteoTracker (Loglisci et al. 2024) measures several meteorological variables, including air temperature, relative humidity, and air pressure. GPS functionality is provided by the connected smartphone, allowing the measured data to be spatially allocated for mapping of heat islands or conducting field research in remote areas.

The vehicle – whether a bicycle or a car – equipped with MeteoTracker should maintain a minimum speed of 7 km/h to ensure adequate airflow and proper ventilation of the sensor. Connected via Bluetooth to a smartphone, it sends readings to an interactive platform through the MeteoTracker app (free for iOS and Android). Users can keep their data private or share it publicly on the MeteoTracker dashboard (https://meteotracker.com/). MeteoTracker is used in several CS projects (e.g. Koedel et al. 2024) and in practical applications such as disaster management and traffic monitoring. In contrast to the SenseBox, which is a customizable do-it-yourself toolkit with modular components, MeteoTracker is ready to use out of the box and designed for ease of application.

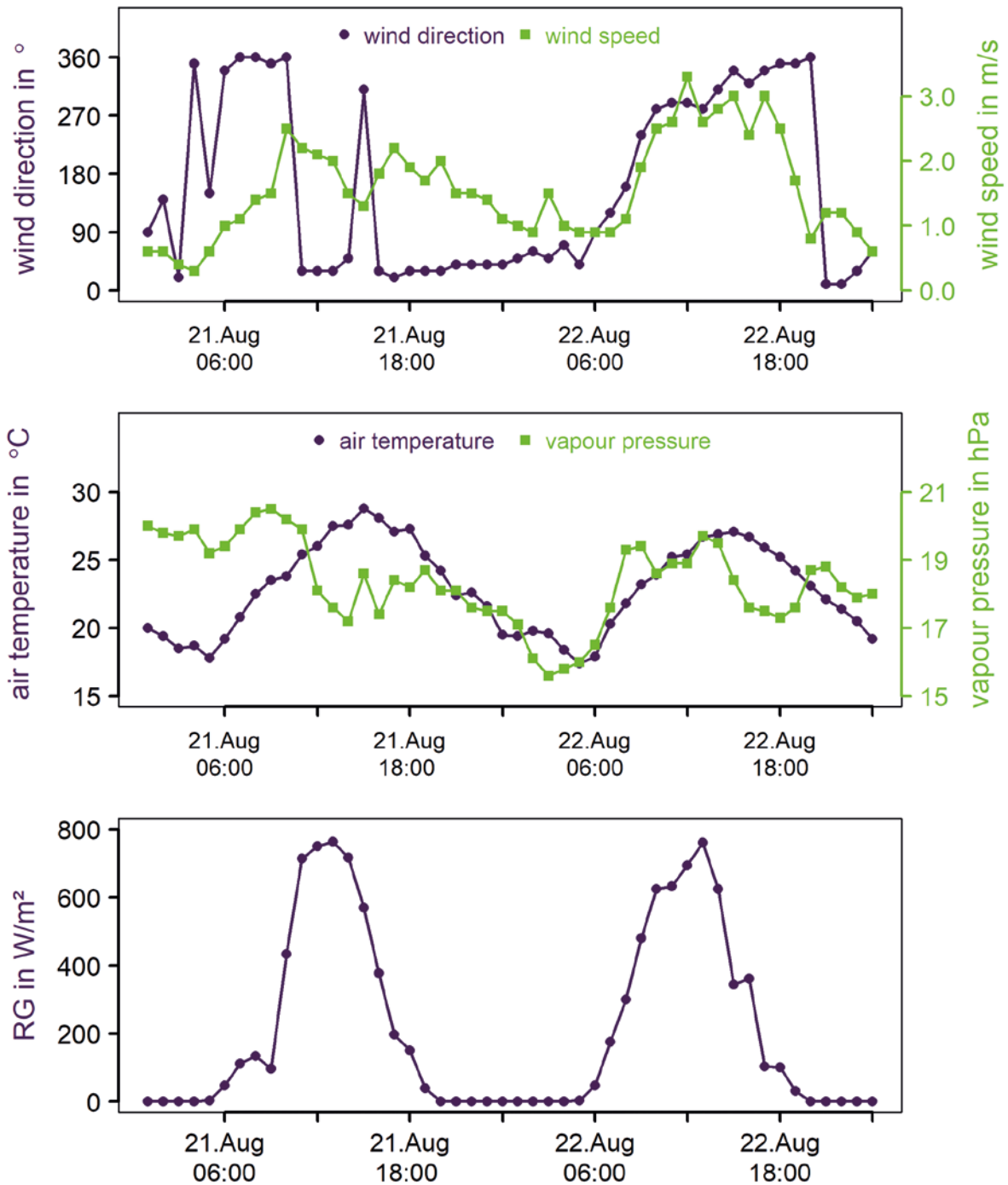

Fig. 2. Hourly data of wind direction, wind speed, air temperature, vapour pressure and global radiation (RG). Source: German Meteorological Service (Deutscher Wetterdienst, DWD), station Leipzig-Holzhausen (wind direction, wind speed, air temperature, vapour pressure) and station Leipzig/Halle Airport (RG). Time is Central European Time (CET).

During the campaign we used three MeteoTracker units on bicycles and one unit installed on a car. Additionally, one bicycle was equipped with a SenseBox. All bicycle tours started and ended at the professional climate station "open area" (Fig. 1 and Fig. 6b).

Ensuring comparability of measurement routes is crucial when comparing mobile measurements from different devices. This is especially challenging when different carrier systems are used, as they move at different speeds and cannot sample all areas equally due to traffic regulations. The

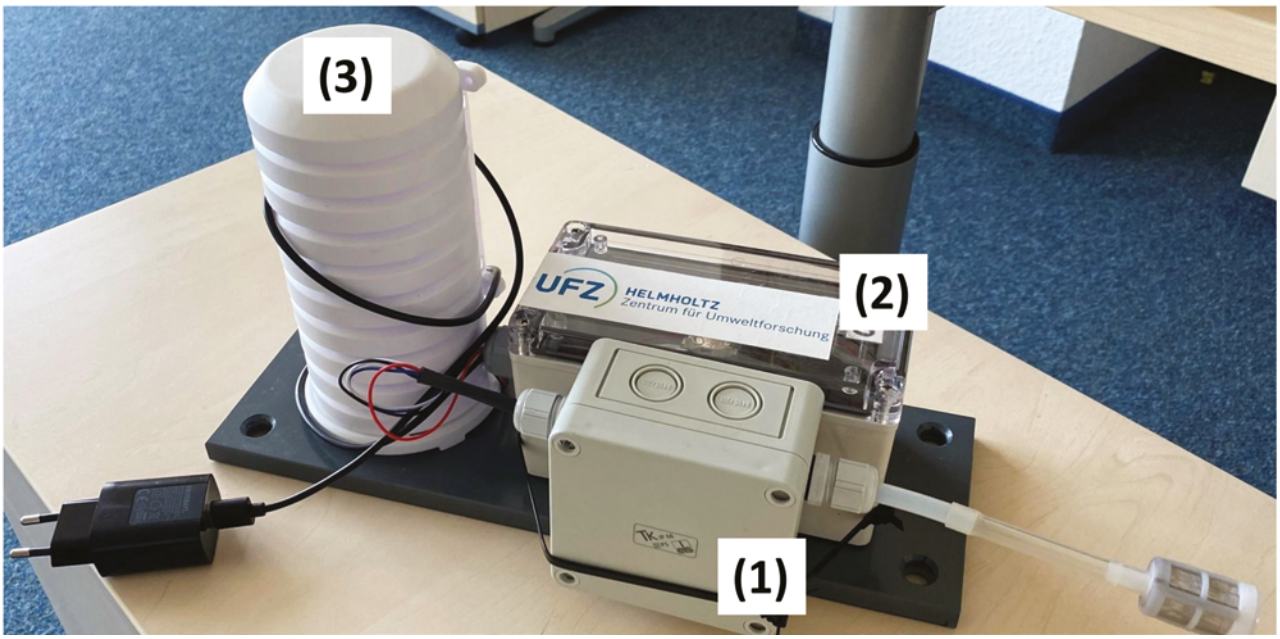

Fig. 3. SenseBox system with (1) dust sensor unit, (2) central microcontroller unit, and (3) radiation shelter housing the air-property sensors (Photo by C. Schütze (UFZ)).



Fig. 4. MeteoTracker installed on a bike running with the smartphone app (Photo by: C. Schütze (UFZ)).

backpack route, designed to cover both sections of the growing urban forest and streets with varying orientations, served as a basis for the bike route. Additionally, comparability with the car route also had to be ensured. Consequently, the bicycle transects largely followed the backpack survey route, while additionally incorporating segments surveyed by car. On selected campaigns, two bicycles and a car were operated in parallel to enable a systematic assessment of inter-device comparability. In total, we conducted 46 tours with the MeteoTracker and on 13 tours with the SenseBox.

2.3.2 Mobile system using a backpack

The backpack was equipped with different measurement devices (Fig. 5). It allowed measurements of air temperature,

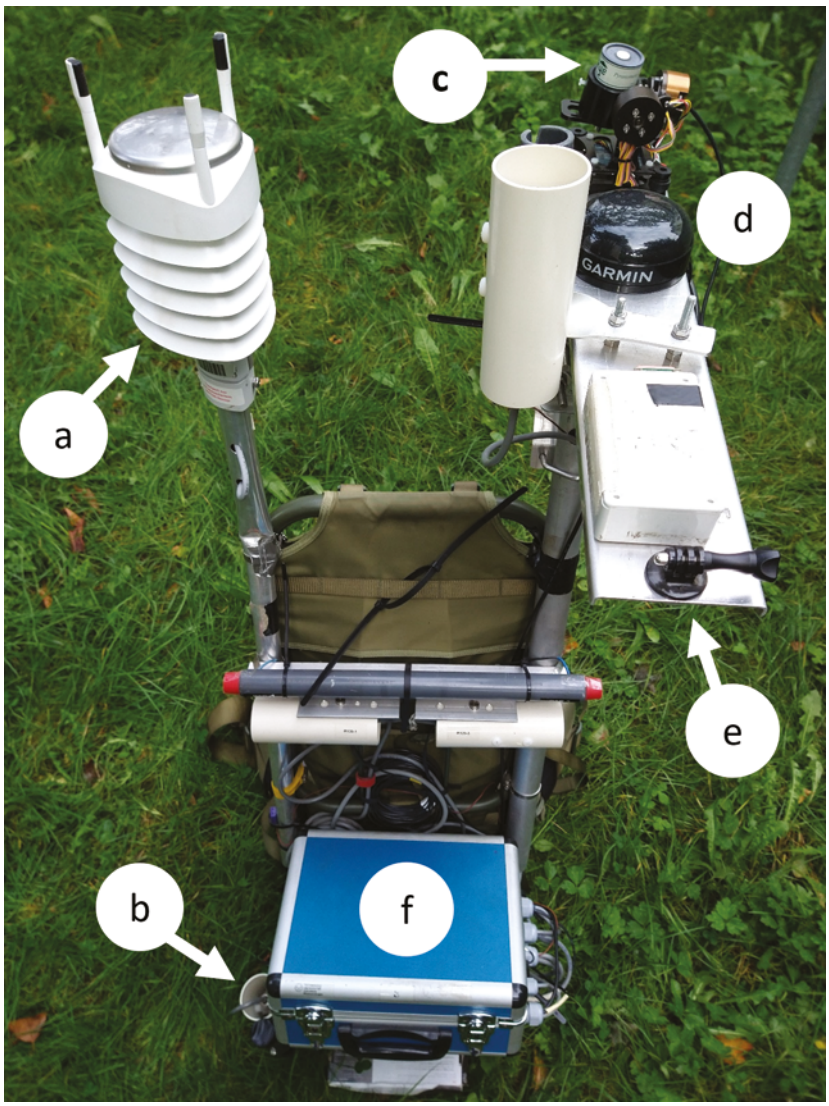

Fig. 5. Used backpack equipment, a: air humidity, air temperature, wind, b: ground surface temperature, c: incident shortwave radiation, d: GPS, e: mounting for GoPro, f: data logger protected in a box (Photo by: U. Moderow, TU Dresden).

air humidity, downward shortwave radiation, wind speed, and surface temperature of the ground. A GPS receiver supplied information concerning position and time and was further used to synchronise all measurements. Measurements were logged every 2 s. However, the GPS signal was often weak or occasionally absent. This caused an uneven distribution of the measurement points along the measurement route and some data loss, particularly during hours of high humidity. A GoPro camera recorded environmental conditions of the lower and upper hemisphere along the measurement track. Due to insufficient power supply, not all measurement walks could be recorded by the GoPro. The same measurement set-up has been used in Moderow et al. (2023).

Measurement walks started and ended at the professional climate station "open area" (Fig. 1, Fig. 6b) and took about 75 minutes each. In total, 12 measurement walks were conducted: five on the 21 August 2023 and six on 22 August 2023.

2.4 Stationary measurements

2.4.1 Bresser-Weather-Station

The NATIONAL GEOGRAPHIC Wi-Fi Colour Weather Station (Bresser GmbH, Germany) with 7-in-1 Sensor by Bresser (Fig. 6a) is a low-cost all-in-one weather station with sensors measuring wind speed, wind direction, humidity, air temperature, rainfall, UV levels, and light intensity. It is widely used and due to its data quality and the user-friendly installation, the weather station is suitable for deployment in CS cases. The Wi-Fi feature allows users to share the data on weather platforms such as AWEKAS, Weather Underground or Weather Cloud. During the campaign, several devices were provided to interested citizen scientists living in the study area, who were recruited through local contacts established as part of the CityCLIM project.



Fig. 6. Stationary measurements, a): Bresser Wi-Fi Weather Station, b): Professional climate station in an open area of a former railway goods station. It is labelled as a climate station "open area" in Fig. 1. Please note that the photo of Fig. 6b has already been taken in July 2023 during a dry period. Vegetation in August 2023 was much more vital. Photo of Fig. 6a by F. Schmidt (UFZ) and photo of Fig. 6b by U. Moderow (TU Dresden).

2.4.2 Climate station – professional standard

The professional climate station (Fig. 6b), situated in an open area of a former railway goods station, measured air temperature, relative humidity, incident shortwave radiation, wind speed, and wind direction. Data were collected via a data logger (CR1000X Campbell Scientific, Logan, USA) with a sampling rate of 1 Hz. Data were stored as 10-min averages. Power supply was provided by batteries. The main difference compared to the Bresser-Weather-Station is that it uses sensors typically not deployed in CS due to cost, and thus mainly used in funded research or commercial applications. Such sensors are usually tested for long-term stability and calibrated with calibration sheets, which increases costs. It should be noted that wind measurements were only available during the measurement campaign and only until the early afternoon on the 22 August 2023. The corresponding devices had to be dismantled due to logistical reasons and as a precautionary against vandalism, since the station was left unattended.

2.5 Overview of all measured variables – mobile systems and stationary systems

Table 1 provides an overview of the systems and the measured variables. Information on the specifications and manufacturer of each device is given in the appendix (Tables A1-A5). Fig. 1 depicts the measurement routes and the location of stationary measurements.

All three mobile devices differ in cost. The total cost of the TU Dresden backpack components is around 8,500 USD, representing a relatively high-priced backpack system, whereas a MeteoTracker costs approx. 350 USD and a SenseBox around 95 USD.

2.6 Methods for air temperature data comparison

Stationary air temperature data were compared with air temperature data obtained through mobile measurements. This comparison was conducted using time series plots. Additionally, measurements obtained from the mobile platforms were evaluated against those from the fixed station "open area" (see Fig. 1 and Fig. 6b).

For the comparison with the "open area" station, only measurements from the backpack and MeteoTracker, and SenseBox systems mounted on bicycles were used. We furthermore considered only those measurements recorded within a 30 m radius of the fixed "open area" station. This spatial constraint reduces the influence of local environmental variability, allowing for a reliable comparison between the sensor systems. MeteoTracker data collected from the car-based setup were excluded, as the "open area" station could not be accessed by car. In the case of the backpack measurements, short stationary measurements beside the station "open area" at the start and end of each walk were used.

To compare the measurements with those from the "open area" climate station, we used scatter plots, the Pearson correlation coefficient and the root mean square error to assess similarities in relative trends and absolute differences, respectively. It should be noted that the averaging time intervals differed between the measurement systems. Ten-minute averages were available for the climate station "open area", whereas the mobile systems used much shorter averaging times, typically under two minutes. Furthermore, the distance covered by the bicycles within the 30 m radius around the fixed station varied

Table 1. Overview of the systems and the measured variables. T_{air} – air temperature, rH – relative humidity, U – wind speed, w_{dir} – wind direction, T_{surf} – surface temperature of the ground, SW_{in} – incident shortwave radiation (upper hemisphere).

	Measured variables									
System	**T_{air}**	**rH**	**U**	**w_{dir}**	**T_{surf}**	**SW_{in}**	**Number of used devices**	**Number of tours**	**Start**	**End**
stationary measurements										
Bresser Wi-Fi Weather Station	x	x	x	x	x	x	2	-	14.08.23	30.08.23
Climate station "open area"	x	x	x	x	-	x	1	-	07.06.23	09.09.23
mobile measurements										
MeteoTracker	x	x	-	-	-	-	4 (3 on bike, 1 on car)	46	18.08.23	22.08.23
Sensebox	x	x	-	-	-	-	1	13	21.08.23	22.08.23
Backpack	x	x	x	-	x	x	1	12	21.08.23	22.08.23

slightly between measurement rounds. To assess whether these differences – in averaging intervals and in covered distances – affected the agreement with the fixed station, we compared the air temperature differences between the mobile systems and the station "open area" with respect to averaging intervals and the distance covered by the bicycles.

In a further step, the LCZ framework was used to categorise the measurement environments. This enabled an investigation into how different urban structural settings may influence the temperature differences observed across measurement systems. In contrast to the comparison with the station "open area", this LCZ- based analysis also included mobile data from the MeteoTracker, which were collected by car.

Data from the MeteoTracker and SenseBox showed unrealistically high air temperature values when the corresponding platform was stationary. These data were excluded from the analysis. (c.f. Chapter 3.1).

2.7 Calculation of UTCI

The Universal Thermal Climate Index (UTCI, Błażejczyk et al. 2010; Bröde et al. 2012; Havenith et al. 2012; Jendritzky et al. 2012) is a human bioclimatic index for assessing thermal comfort. Its unit is degree Celsius, and different levels of thermal stress are distinguished, ranging from extreme cold stress to no thermal stress to extreme heat stress. The following variables, all recorded by the backpack, were used to calculate the UTCI: global radiation (W m^{-2}), air temperature (°C), relative humidity (%), wind speed (m s^{-1}) and ground surface temperature (°C).

We used RayMan Pro 2.2 (Matzarakis et al. 2010) to obtain UTCI values. RayMan Pro 2.2 applies a regression equation for the UTCI (Bröde et al. 2012 and therein cited online resources).

The movement of the measuring backpack caused by the carrier influences the wind speed measurement. Therefore, the wind was set to the minimum value (0.5 m/s) in the RayMan calculation. As the wind field within a city is variable, the resulting UTCI values are slightly overestimated when using this fixed value. However, the temporal evolution and spatial distribution are still well represented.

In the following, the term "heat stress" primarily refers to climatic exposure, i.e., the magnitude and spatial distribution of atmospheric conditions such as air temperature and UTCI.

2.8 Heat stress and citizen science

Measuring air temperature distribution within cities by engaging people via CS has been undertaken by several studies (Fenner et al. 2017; Marquès et al. 2022; Meier et al. 2017). However, heat stress does not solely depend on air temperature but also on radiation, moisture, wind and the characteristics of the human being itself (e.g. clothes, activity). The use of air temperature (T_{air}) or surface temperature (T_{surf}) as a proxy for heat stress has been criticised, but it remains widely used because these variables can be measured relatively easily, and spatial information is available via satellites in the case of T_{surf} (e.g. Dugord et al. 2014; Goldblatt et al. 2021; Zhou et al. 2019).

Here, we investigate how heat stress, expressed as UTCI, relates to T_{air} and T_{surf}. For this purpose, we analysed two backpack measurement walks. The first walk in the late morning on 21 August 2023, took place under conditions of high heat stress, while the second walk in the early morning on 22 August 2023 took place under conditions of low or no heat stress. We calculated the correlations between UTCI, T_{air} and T_{surf} to examine the relationship between them. This was done for both measurement walks.

To enable comparison of the variability observed during the walks, each variable was normalised by its maximum value of the respective walk. We also examined potential differences in the variability of these quantities (T_{air}, T_{surf},

and UTCI) within a local climate zone as this framework is increasingly used also by authorities and interested citizens (Ching et al. 2018; Lehnert et al. 2021a; Yang et al. 2025). We selected LCZ 5 (open mid-rise) for this purpose as it showed the best coverage by the backpack walks.

3 Results and discussion

This section addresses the research questions outlined in the introduction, with a particular emphasis on T_{air} as the primary variable under investigation. The results first explore the performance of different systems by evaluating their ability to capture temporal patterns. Measured T_{air} from the different mobile systems were compared to assess both the advantages (e.g., cost-efficiency) and the challenges (e.g., data consistency) of CS relative to professional measurements. Additionally, we discuss the practical implications for the establishment of guidelines within the framework of CS. Differences and similarities in the spatial distribution and characterisation of heat stress are discussed when T_{air} or T_{surf} is used instead of a human bioclimatic index (here, UTCI). The LCZ concept is applied to classify the mobile measurements, i.e. to compare the influence of environmental conditions on the measured variables.

3.1 Comparison of different mobile measurements and different stationary measurements

We analysed the temporal patterns of both stationary and mobile measurements. Fig. 7 shows a comparison of T_{air} measurements from stationary and mobile sensors between 21 and 22 August 2023. T_{air} (in °C) is plotted on the y-axis, while Central European Time (CET) is shown on the x-axis. Different measurement methods and devices are included: continuous T_{air} data from fixed locations provided by two professional stations, "DWD Leipzig-Holzhausen" and "open area", as well as the CS station "Bresser". In addition, T_{air} readings from the mobile systems – MeteoTracker and SenseBox mounted on bicycles and the backpack – are shown (averages of measurements obtained in the vicinity of the station "open area", c.f. chapter 2.6).

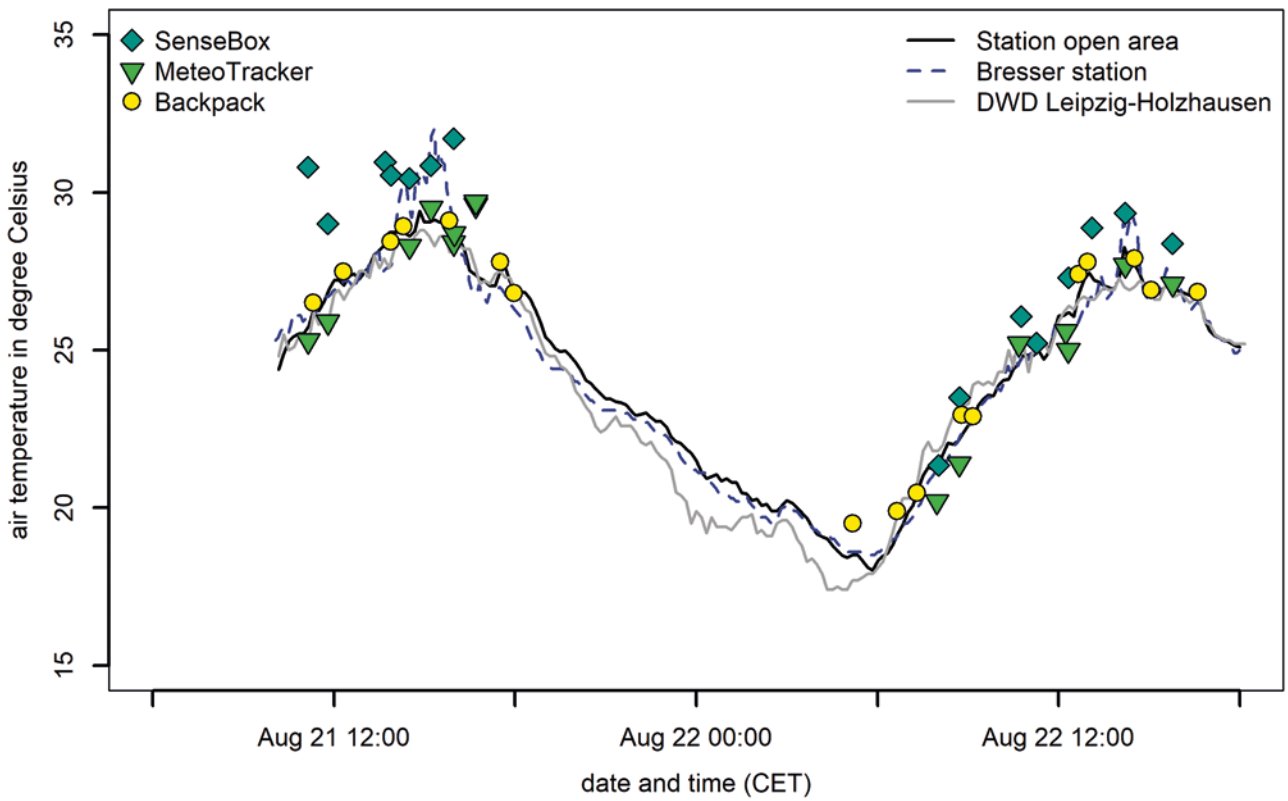

Fig. 7. Stationary measurements of T_{air} at three different stations (lines, German Meteorological Service DWD station in Leipzig-Holzhausen, professional climate station "open area" and Bresser station) compared with mean T_{air} recorded by the three different mobile systems (symbols). Values of mobile systems were obtained by stationary measurements adjacent to the climate station "open area" (backpack) and within a distance of 30 m around the "open area" climate station when the corresponding bicycles passed by according to their measurement route (SenseBox, MeteoTracker).

The continuous stationary measurements provide consistent, high-precision data at fixed locations. The three stationary datasets closely follow similar temperature trends, indicating stable and reliable measurements with minor fluctuations. This consistency suggests that the fixed locations experience a relatively uniform temperature pattern, with only small variations. However, the data obtained by the CS station (Bresser) deviates slightly from the others, especially during periods of high T_{air} between 14:00 and 15:00 CET on both days.

On both days, the mobile measurements generally followed the course of the stationary observations. While the MeteoTracker and backpack values remained largely consistent with those of the fixed stations, the SenseBox tended to record slightly higher temperatures than the stationary devices. To further analyse the agreement with the "open area" station, we utilised scatter plots (Fig. A1, A2, A3 in the Appendix) and statistical measures (Table 2).

As shown in Fig. 7, the correlation coefficient indicates that the relative course between the mobile systems and the professional station "open area" aligns closely. Additionally, the RMSE values indicate differences in the absolute values between the fixed station and the mobile measurements. These differences increase from the backpack to the MeteoTracker and further to the SenseBox. It should be noted that discrepancies exist between the analysed time intervals. Ten-minute averages were available for the station "open area" whereas averaging times varied for the mobile systems (usually clearly less than two minutes). We checked whether the slightly different averaging intervals and covered distances (in the case of the MeteoTracker and the SenseBox) might have affected the agreement with the fixed station. In neither case was a clear dependency detectable. Therefore, we assume that the different averaging times and slight differences in the covered distance (MeteoTracker and SenseBox) only have a minor impact on the results obtained.

Table 2. Comparison of T_{air} data of the fixed station "open area" to T_{air} data recorded by the backpack, SenseBox, and MeteoTracker, respectively. r denotes correlation coefficient and RMSE denotes root mean square error.

	backpack	MeteoTracker	SenseBox
Number of data pairs	17	16	15
r	+ 0.99	+ 0.93	+ 0.93
RMSE in °C	0.42	1.05	2.08

Notably, during peak daytime temperatures, the mobile sensors – especially the SenseBox – tend to record slightly higher temperatures than the stationary devices. These deviations are likely due to insufficient sensor ventilation, which makes low-cost devices more susceptible to radiation-induced heating. Fig. 8 illustrates this effect, showing MeteoTracker measurements including a brief stop at a traffic light. This interruption, which temporarily reduced ventilation, led to artificially elevated T_{air} values.

The issue of insufficient ventilation was strongly observed for the low-cost device SenseBox, which resulted in unreliable data and ultimately led to its exclusion from the subsequent analyses.

During the early morning hours, the temperatures recorded by mobile and stationary systems align very closely, with few significant differences. This pattern suggests that, during periods of moderate T_{air}, both mobile and stationary devices capture consistent and comparable ambient T_{air}. During nighttime, the DWD weather station recorded the lowest air temperature values among all stationary stations, likely due to its more rural location on the outskirts of Leipzig (Behrens & Hoffmann 2016). This suggests that it is less affected by the urban heat island effect.

Our results are partly in line with previous works, which evaluate the quality of used mobile CS devices. The performance of MeteoTracker was assessed in recent studies (Antoniciello 2021; Barbano et al. 2024; Loglisci et al. 2024). Antoniciello (2021) evaluates measurements using MeteoTracker by cars and bicycle. For the measurements with a bicycle, an evening measurement run is shown, which represents the spatial temperature distribution of an area in Turin

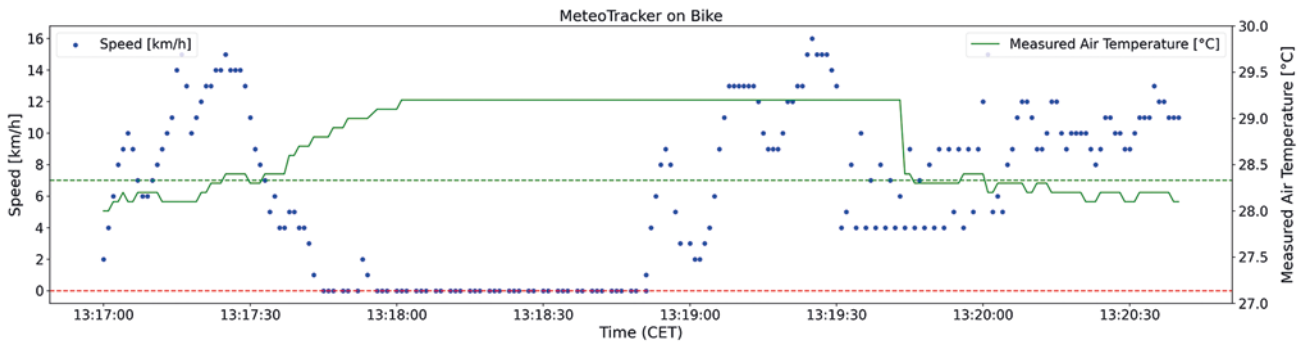

Fig. 8. Example for a disturbed T_{air} measurement due to a short stop at a traffic light. When the speed drops below 7 km/h (green dotted line), the ventilation of the MeteoTracker becomes unreliable, affecting the accuracy of the temperature measurement. When the bike stops (speed = 0 km/h, red dotted line), the measured temperature rises due to reduced airflow and radiation heat. When the bike starts moving again, the temperature measurements take some time to return to its original level, indicating a lag in the system's response.

but possible radiation errors are not addressed (Antoniciello 2021). It is concluded that MeteoTracker is generally suitable for mobile measurements, but it is recognised at the same time that further analyses are necessary. Barbano et al. (2024) evaluated the MeteoTracker device in detail for stationary and mobile measurements. They found an overestimation of T_{air}, which slightly increased with higher levels of incident solar radiation, based on measurements conducted in early spring in the Netherlands. Their conclusion is that, as long as the required working conditions for the MeteoTracker are met, reliable measurements can be obtained. A similar conclusion is drawn by Loglisci et al. (2024), but neither investigate summer conditions. In contrast to these works, we measured under summer conditions with very high irradiation.

Generally, current literature is sparse concerning T_{air} measurements by SenseBox devices. Schmidt et al. (2023) investigated different low-cost CS devices for mobile measurements, including SenseBox, and noted that insufficient ventilation can affect measurement results. Our results emphasise the need to comply with the specified conditions for using the MeteoTracker especially during periods of high incident radiation. Similarly, sufficient ventilation must be ensured when using the SenseBox. This aspect should be incorporated into CS guidelines.

In a further step we investigated how the measured T_{air} of the different mobile systems varied across different local climate zones.

Fig. 9 shows that all datasets obtained via backpack, bicycle (only MeteoTracker), and car consistently covered the same narrow temperature range. However, the boxplot also illustrates pronounced differences in temperature measurements depending on the platform used. Backpack measurements consistently show the highest values and the largest variability across all investigated LCZ classes. Bike measurements fall in the intermediate range, whereas car-based measurements consistently show least variable and mostly lowest temperatures. Various factors contribute to this result.

Backpack surveys are conducted at a slow pace, recording differing microclimatic conditions along the route in more detail. This contributed to higher variability in the T_{air} data collected by the backpack. Mobile surveys conducted by bicycles and cars move at higher speeds and therefore cannot capture local conditions in as much detail as backpack measurements, resulting in temperature data with lower variability. The higher speed of these two platforms also likely reduced the influence of radiation exposure and insufficient ventilation, provided the minimum speed required for sufficient ventilation of the measurement equipment was maintained. This might have favoured lower maximum values for the bicycle and car surveys.

In addition, route accessibility was limited for cars and, to a lesser extent, for bike surveys, whereas backpack surveys could access narrow urban areas and local heat hotspots, which may have contributed to the higher variability and higher recorded values of the backpack. Additionally, partly differing routes within a given LCZ may have contributed to the difference in variability and maximum values.

T_{air} measurements of the respective measurement systems were not trend-corrected. This means that the influence of the different measurement route durations (backpack vs.

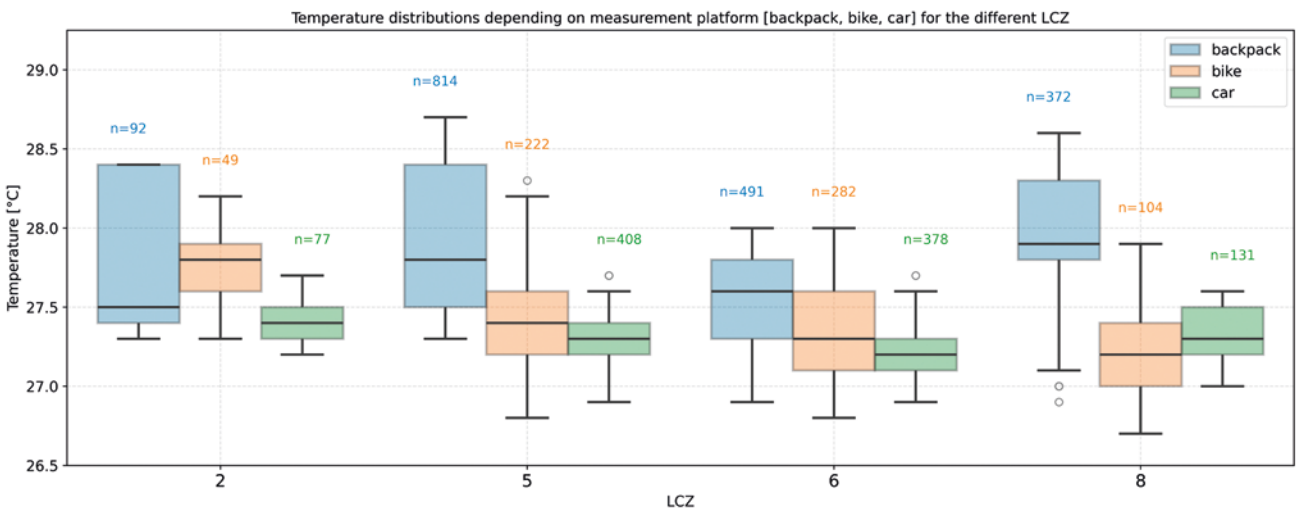

Fig. 9. Boxplots of T_{air} measurements across the covered local climate zones obtained in the same temporal measurement window on 22.08.23 12–14:30 CET, differentiated by measurement platform (backpack, bike, car). Backpack surveys show the highest values and largest variability, reflecting stronger influences of radiation exposure, insufficient ventilation, slower measurement speed, and access to narrow urban areas and local heat hotspots. Car-based measurements yield the lowest and most stable temperatures due to higher speed, stronger ventilation, and limited route accessibility, with bike data generally falling in between. Overall, platform-specific effects and accessibility constraints overlay the variation between LCZ classes. (Numbers n above each box indicate the amount of individual measurements underlying the respective distribution.).

car) and the associated temperature trends also becomes apparent in the statistical analysis.

Obtained pattern of Fig. 9 indicates that the measurement environment, particularly air flow and shading in mobile systems, data acquisition duration, and moving speed have a substantial impact on the recorded T_{air}.

According to the application guidelines by Parlow & Foken (2021), Table 3 summarises the characteristic features of the platforms used. The backpack platform is tailored for scientific applications and provides numerous high-quality data streams that enable detailed insights into structural temperature patterns. However, its operation is more complex and requires expert knowledge. In contrast, MeteoTracker devices, commonly used in CS projects, are highly flexible and, when applied correctly and accompanied by appropriate quality control, can generate data of sufficient quality for scientific purposes. Their main advantage is the ability to cover large areas within a short time when mounted on vehicles, thereby providing an overview of urban T_{air} conditions. A potential limitation of the MeteoTracker mobile sensing systems lies in the observed variability of data point density, which we encountered during our measurement campaign. As mentioned in section 2.3.1, the spatial resolution of recorded data is influenced by the smartphone GNSS sensor and its operating system. In comparative tests, iPhones (iOS) produced a point density roughly three times higher than Android devices (e.g., Samsung phones) along identical tracks.

3.2 Heat stress and citizen science

The following analyses compare the suitability of T_{air} and T_{surf} as proxies for human heat stress, assessed using the UTCI. Two measurement walks were analysed: one under low-radiation conditions in the early morning (22.08.2023, 05:09–06:36 CET) and one under high-radiation conditions in the late morning (21.08.2023, 09:33–11:17 CET).

UTCI exhibits a stronger association with T_{air} under low-radiation conditions, whereas under high-radiation regimes it aligns more closely with T_{surf} (Table 4). This pattern reflects the shared sensitivity of UTCI and T_{surf} to incident shortwave radiation during daytime, in contrast to nocturnal conditions when longwave radiative fluxes dominate the surface–atmosphere energy balance. As the variables were not trend-adjusted, the weaker relationship between T_{air} and UTCI during the early morning walk likely reduced their correlation.

To compare the variability along the measurement paths, all variables were normalised by their respective maximum values (Fig. 10). T_{surf} exhibits the highest variability, T_{air} the lowest, with UTCI in between. Variability is higher during daytime under high-radiation conditions, particularly for T_{surf} and UTCI, due to rapidly changing radiation conditions (sunlit and shadowed areas) and heterogeneous surface characteristics (e.g. albedo and heat capacity).

Beyond differences in variability and timing, an important question is whether T_{air} and T_{surf} are able to reproduce

Table 3. Comparison of characteristic features of the three measurement platforms used (scientific backpack, MeteoTracker on bike, and MeteoTracker on car).

Characteristic features	BACKPACK	BIKE	CAR
Low Price	-	++	++
Suitability for various user groups	-	+	+
Possibility to measure multiple variables	++	+	+
Flexibility to add further sensors	++	-	-
Spatial coverage – Measurement range (distance covered)	-	+	++
Spatial coverage – accessibility to areas under consideration	++	++	-
Temporal coverage – Suitability for long-term measurements	-	-	-
Temporal coverage – Suitability for short-term measurements	++	++	++
Temporal coverage – Suitability for periodic measurements	+	++	++
Positional accuracy[$]	+	+	+
Spatial/temporal resolution	++	+ / depends on velocity and used firmware	
Low installation effort	+	++	++
Low level of required knowledge	+	++	++
Easy handling	+	++	++
Low measurement effort	+	++	++
Low maintenance effort	+	++	++
Real-time data accessibility	-	++	++
Low level of required data processing and quality control	-	-	-
Data quality sufficient for scientific application	++	+	+

[$] Depends on the used GPS system and atmospheric conditions and, if applicable, the operating system of the smartphone used.

Table 4. Relation between UTCI and T_{air} and T_{surf}, respectively for conditions with high radiation (21.08.2023 09:33–11:17 CET) and low radiation (22.08.2023 05:09–06:36 CET) addressed using the coefficient of determination (R^2).

Measurement walk	Number of data pairs	R^2	
		UTCI and T_{air}	UTCI and T_{surf}
21.08.2023 09:33–11:17 CET	1639	0.19	0.63
22.08.2023 05:09–06:36 CET	1473	0.62	0.28

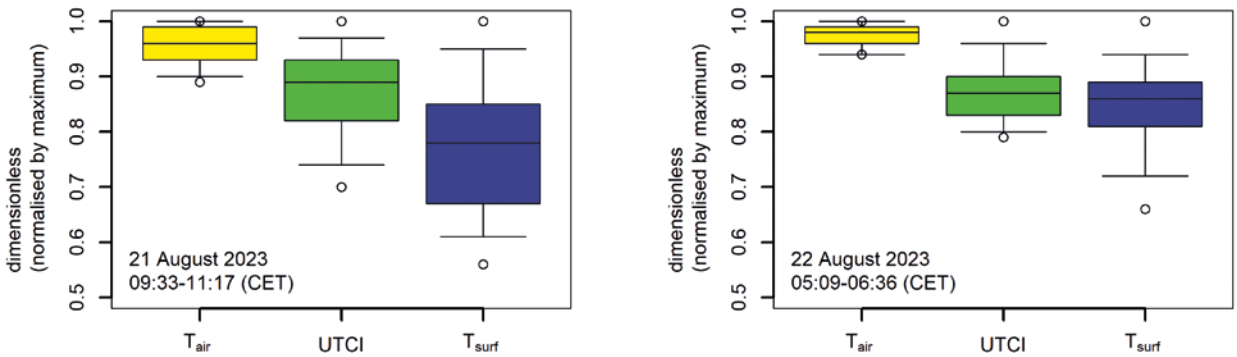

Fig. 10. T_{air}, UTCI, and T_{surf} normalised by its maximum value of the respective walk. The left graph refers to conditions of high radiation, while the right graph shows conditions of low radiation. Boxplots show median (black line), 25th and 75th percentile (ends of boxes), 5th and 95th percentile (whiskers) and maximum and minimum values (open circles). The number of used data points is given in Table 4.

the spatial patterns of heat stress captured by UTCI. Spatial patterns of hot and cool spots differ markedly between the variables (Fig. 11). During high-radiation conditions, several UTCI hot spots, such as along Antonienbrücke and at locations where walking was interrupted to pass a street (Klingenstraße, Gießerstraße), are largely missed by T_{air}. Agreement between UTCI and T_{surf} is better for some hot (along Gießerstraße and Klingenstraße) and cool spots (running from easterly direction to westerly direction), but remains incomplete, especially along Antonienbrücke. During the early morning walk, spatial agreement between UTCI and both T_{air} and T_{surf} is generally weaker, as increasing and spatially heterogeneous shortwave radiation during the transition from night to day leads to less distinct patterns.

While these results refer to spatial patterns along individual measurement paths, Fig. 12 places the observed differences in variability into the context of a specific LCZ. Fig. 12 confirms that within LCZ 5 (Open midrise), T_{air} shows lower variability than UTCI, while T_{surf} shows higher variability and a wider absolute temperature range similar to the results of Chakraborty et al. (2022). Differences in diurnal timing further complicate the use of single variables as proxies. Maximum T_{air} typically occurs later than maximum T_{surf}, as atmospheric warming starts from the surface and is governed by different thermal properties and heat transport processes (Oke 1987). UTCI, being strongly influenced by radiation, often peaks earlier than T_{air}. Consequently, its peak often occurs close to that of T_{surf}, although time shifts may occur depending on atmospheric conditions. Backpack measurements indicate that T_{air} peaked later than both T_{surf} and UTCI, although limited data coverage and intermittent cloudiness restrict quantitative assessment of time shifts.

In summary, UTCI aligns preferentially with T_{air} under low-radiation conditions and with T_{surf} under high-radiation regimes. Nonetheless, T_{air} attenuates while T_{surf} amplifies the spatial variability of heat stress, and both metrics only partially reproduce the UTCI-derived hot and cool spot patterns.

Overall, the results remain robust when a simplified mean radiant temperature parameterization is used to calculate UTCI values, although minor deviations are observed.

Consequently, statements on heat stress variability and the spatial distribution of thermal hot spots are prone to error when based solely on T_{air} or T_{surf} instead of bioclimatic indices. This is consistent with previous studies emphasising that neither T_{air} nor T_{surf} alone can provide a comprehensive representation of human heat stress (Moderow et al. 2023; Stewart et al. 2021).

Empirical evidence further supports this limitation. Lehnert et al. (2021b) showed that areas with very high T_{surf} coincided in less than 50% with locations that city dwellers themselves identified as highly heat stressed, highlighting the risk of misclassification when T_{surf} is used as a proxy for experienced heat stress. While other studies report mixed conclusions regarding the suitability of T_{surf} as a proxy (e.g. Chakraborty et al. 2022; Muse et al. 2024; Anders et al. 2025), our results suggest that the limitations of T_{surf} are more pronounced under nocturnal than under daytime conditions, highlighting the importance of explicitly accounting for radiation effects when assessing human heat stress.

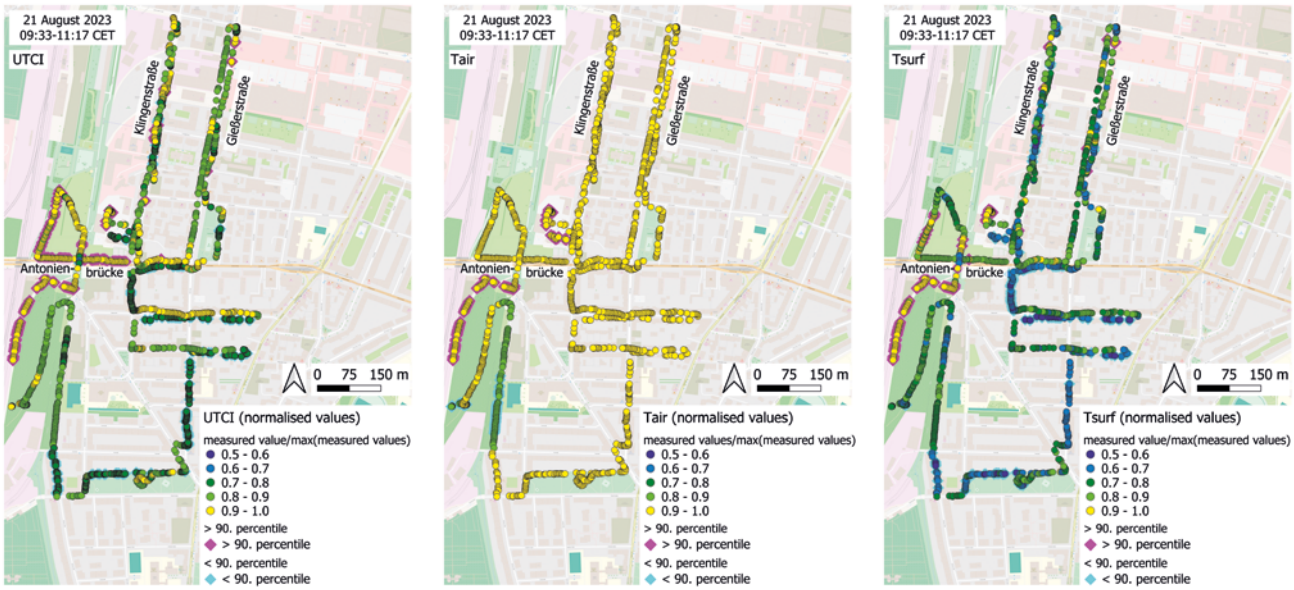

Fig. 11. Normalised UTCI, T_{air}, and T_{surf} (from left to right, normalised by its maximum value of the respective walk).

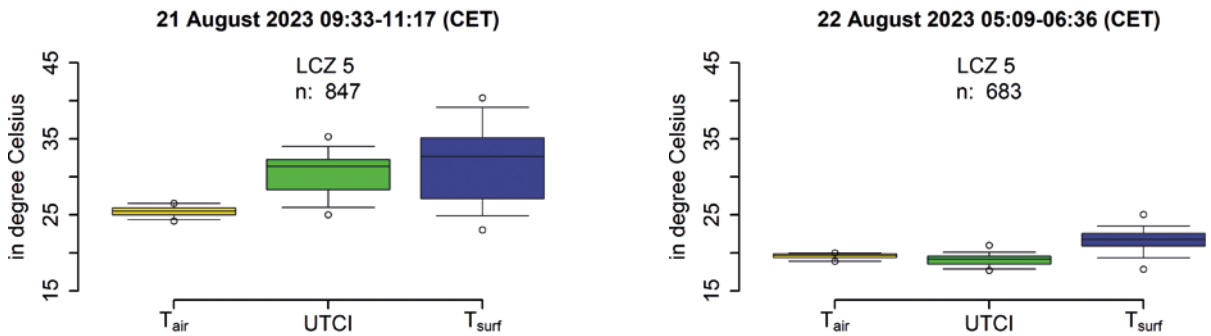

Fig. 12. Variability of UTCI, T_{air}, and T_{surf} as measured in LCZ 5 (Open midrise) by two measurement walks, left: conditions of high radiation, right: conditions of low radiation. Boxplots show median (black line), 25th and 75th percentile (ends of boxes), 5th and 95th percentile (whiskers) and maximum and minimum values (open circles).

Moreover, because T_{air} typically peaks later in the day than T_{surf} and UTCI under high-radiation conditions, periods of maximum heat stress may be incorrectly identified when relying on T_{air} alone. Therefore, CS projects addressing urban heat stress should clearly communicate that, although T_{air} and T_{surf} significantly influence human thermal stress, they cannot be equated with bioclimatic heat stress indices such as UTCI.

4 Summary and conclusions

Mobile measurements of micrometeorological conditions within the city of Leipzig (Germany) were performed during two days with heat stress potential. Different mobile platforms (car, bicycle, pedestrian with backpack) were used alongside stationary measurements. The instruments included those used in CS (MeteoTracker, SenseBox) as well as professional-grade devices. These measurements formed the basis for the subsequent analysis addressing the questions raised.

Our data show that the diurnal cycle of T_{air} can be captured reasonably well by mobile CS measurements compared to a reference station. However, RMSE values indicate that differences in absolute values exist. Different LCZs were assessed by the different mobile systems within the same narrow T_{air} range. Variability in T_{air} was greatest in backpack surveys, lowest in car surveys, and intermediate in bicycle surveys.

Radiation errors became obvious, when the moving speed dropped below the recommended minimum speed. Besides these meteorological aspects, we observed a varying number of data points for the MeteoTracker depending on the operating system of the smartphone used.

A comparison of the spatial variability of T_{air}, T_{surf} of the ground, and heat stress along two selected measurement tracks of the backpack route showed that heat stress is more related to T_{air} during periods of low radiation. During periods of high radiation, heat stress is more closely related to T_{surf}. However, there are marked differences in the location of hot spots among these three variables, and they also differ in their variability.

The variability of T_{air}, T_{surf}, and heat stress within a LCZ also differs. Furthermore, a time shift between the peak values of T_{air} and UTCI was observed. This means that using T_{air} as a proxy for heat stress may result in inaccurately capturing the timing of the highest heat stress exerted by the environment.

Based on these results, we conclude that guidelines for CS measurements should address radiation errors and provide recommendations on how to reduce them. They should also clarify that human heat stress is not equivalent to T_{air} or T_{surf}. However, during periods of low radiation, T_{air} serves as a better proxy for heat stress than T_{surf}, whereas during periods of high radiation, T_{surf}, when available, is a better proxy than T_{air}. Despite these relationships, significant differences can occur in the location of hot spots, as well as in the variability and timing of maximum values. From a technical perspective, the guidelines should note that the number of data points collected by mobile measurements requiring a smartphone may depend on the smartphone's settings and operating system.

With respect to LCZs, CS can contribute to expanding the database for a better description of LCZs based on T_{air}, as this is a commonly measured variable by CS instruments. This provides an opportunity to study variability within LCZs by filling data gaps, engaging communities, and improving urban climate assessments. It is suggested that measurements should be taken in the late evening or early morning hours to better capture differences between LCZs. This timing also aligns with a primary application of LCZs: mapping the urban heat island during low-radiation periods. In addition, windless and cloudless conditions are preferred as local differences become more apparent, allowing for better distinction between LCZs.

Besides this, it would be worthwhile to examine whether the globally available LCZ framework is suitable for mapping significant differences under daytime conditions, and whether these differences are transferable to other cities. Such an approach would require sufficient data for all LCZs, as well as a measurement concept specifically designed for this purpose.

Acknowledgement: We would like to thank the students Marius Döbberthin and Chris Burschyk (both TU Dresden) and the student Fabian Schütze (UFZ) for their help and enduring support during the two-day mobile measurements. The Urban Forest project ('URBANE WÄLDER') was funded by the Federal Agency for Nature Conservation of the Federal Republic of Germany. CityCLIM project has received funding from the European Union's Horizon 2020 research and innovation programme under grant agreement No 101036814. Special thanks go to two anonymous reviewers for their time and valuable comments, which greatly helped to improve the manuscript.

References

Anders, J., Schubert, S., Maronga, B., & Salim, M. (2025). Simplifying heat stress assessment: Evaluating meteorological variables as single indicators of outdoor thermal comfort in urban environments. *Building and Environment, 274*, 112658. https://doi.org/10.1016/j.buildenv.2025.112658

Antoniciello, G. (2021). MeteoTracker, una piccola ma promettente stazione meteo portatile. *Nimbus, 86*, 6–9.

Barbano, F., Brattich, E., Cintolesi, C., Ghafoor Nizamani, A., Di Sabatino, S., Milelli, M., … Parodi, A. (2024). Performance evaluation of MeteoTracker mobile sensor for outdoor applications. *Atmospheric Measurement Techniques, 17*(10), 3255–3278. https://doi.org/10.5194/amt-17-3255-2024

Beck, D., & Mitkiewicz, J. (2025). A systematic literature review of citizen science in urban studies and regional urban planning: Policy, practical, and research implications. *Urban Ecosystems, 28*(2), 85. https://doi.org/10.1007/s11252-025-01693-8

Behrens, U., & Hoffmann, K. (2016). *Bericht – Stadtklimatische Untersuchungen in Leipzig. Ergebnisse statistischer Auswertungen langjähriger Klimareihen sowie temporärer Stations- und Profilmessungen.* Potsdam: Deutscher Wetterdienst. https://www.dwd.de/DE/klimaumwelt/klimaforschung/klimawirk/stadtpl/stadtklimaprojekte/projekt_leipzig/externe_links/ergebnisse.pdf?__blob=publicationFile&v=2

Błażejczyk, K., Broede, P., Fiala, D., Havenith, G., Holmér, I., Jendritzky, G., … Kunert, A. (2010). Principles of the New Universal Thermal Climate Index (UTCI) and its Application to Bioclimatic Research in European Scale. *Miscellanea Geographica, 14*(1), 91–102. https://doi.org/10.2478/mgrsd-2010-0009

Bröde, P., Fiala, D., Błażejczyk, K., Holmér, I., Jendritzky, G., Kampmann, B., … Havenith, G. (2012). Deriving the operational procedure for the Universal Thermal Climate Index (UTCI). *International Journal of Biometeorology, 56*(3), 481–494. https://doi.org/10.1007/s00484-011-0454-1

Chakraborty, T., Venter, Z. S., Qian, Y., & Lee, X. (2022). Lower Urban Humidity Moderates Outdoor Heat Stress. *AGU Advances, 3*(5), e2022AV000729. https://doi.org/10.1029/2022AV000729

Ching, J., Mills, G., Bechtel, B., See, L., Feddema, J., Wang, X., … Theeuwes, N. (2018). WUDAPT: An Urban Weather, Climate, and Environmental Modeling Infrastructure for the Anthropocene. *Bulletin of the American Meteorological Society, 99*(9), 1907–1924. https://doi.org/10.1175/BAMS-D-16-0236.1

Demuth, D., Nuest, D., Bröring, A., & Pebesma, E. (2013). *The AirQuality SenseBox*. EGU2013-5146.

Demuzere, M., Bechtel, B., Middel, A., & Mills, G. (2020). *European LCZ map* [Data set]. https://figshare.com/articles/dataset/European_LCZ_map/13322450

Demuzere, M., Bechtel, B., Middel, A., & Mills, G. (2019). Mapping Europe into local climate zones. *PLoS One, 14*(4), e0214474. https://doi.org/10.1371/journal.pone.0214474

Dugord, P.-A., Lauf, S., Schuster, C., & Kleinschmit, B. (2014). Land use patterns, temperature distribution, and potential heat

stress risk – The case study Berlin, Germany. *Computers, Environment and Urban Systems, 48*, 86–98. https://doi.org/10.1016/j.compenvurbsys.2014.07.005

Fenner, D., Meier, F., Bechtel, B., Otto, M., & Scherer, D. (2017). Intra and inter 'local climate zone' variability of air temperature as observed by crowdsourced citizen weather stations in Berlin, Germany. *Meteorologische Zeitschrift (Berlin), 26*(5), 525–547. https://doi.org/10.1127/metz/2017/0861

Gallinelli, P., Camponovo, R., & Guillot, V. (2017). CityFeel – Micro climate monitoring for climate mitigation and urban design. *Energy Procedia, 122*, 391–396. https://doi.org/10.1016/j.egypro.2017.07.427

Goldblatt, R., Addas, A., Crull, D., Maghrabi, A., Levin, G. G., & Rubinyi, S. (2021). Remotely Sensed Derived Land Surface Temperature (LST) as a Proxy for Air Temperature and Thermal Comfort at a Small Geographical Scale. *Land (Basel), 10*(4), 410. https://doi.org/10.3390/land10040410

Gracia-León, H., Restrepo, E. G., Uribe-Jongbloed, A., & Urrego, L. R. (2021). Mobile Environmental Measurement Laboratory Using Electric Vehicles for Smart Cities. In F. Trapani, N. Mohareb, F. Rosso, D. Kolokotsa, S. Maruthaveeran, & M. Ghoneem (Eds.), *Advanced Studies in Efficient Environmental Design and City Planning* (pp. 429–436). Cham: Springer International Publishing; https://doi.org/10.1007/978-3-030-65181-7_34

Hagemann, R., Corsmeier, U., Kottmeier, C., Rinke, R., Wieser, A., & Vogel, B. (2014). Spatial variability of particle number concentrations and NOx in the Karlsruhe (Germany) area obtained with the mobile laboratory 'AERO-TRAM'. *Atmospheric Environment, 94*, 341–352. https://doi.org/10.1016/j.atmosenv.2014.05.051

Havenith, G., Fiala, D., Błazejczyk, K., Richards, M., Bröde, P., Holmér, I., … Jendritzky, G. (2012). The UTCI-clothing model. *International Journal of Biometeorology, 56*(3), 461–470. https://doi.org/10.1007/s00484-011-0451-4

Heusinkveld, B. G., Steeneveld, G. J., van Hove, L. W. A., Jacobs, C. M. J., & Holtslag, A. M. (2014). Spatial variability of the Rotterdam urban heat island as influenced by urban land use. *Journal of Geophysical Research. Atmospheres, 119*(2), 677–692. https://doi.org/10.1002/2012JD019399

Hoffmann, K., & Kreienkamp, F. (2019). *Stadtklimatische Untersuchungen in Halle (Saale) Auswertung von Klimamessungen und Modellsimulationen für die Vergangenheit, Gegenwart und Zukunft. DWD Synthesebericht* [DWD Synthesebericht]. https://www.dwd.de/DE/klimaumwelt/klimaforschung/klimawirk/stadtpl/publikation_stadtplanung/pdf/dwd_synthesebericht.html

Hooyberghs, H., De Craemer, S., Lefebvre, W., Vranckx, S., Maiheu, B., Trimpeneers, E., … Fierens, F. (2022). Validation and optimization of the ATMO-Street air quality model chain by means of a large-scale citizen-science dataset. *Atmospheric Environment, 272*, 118946. https://doi.org/10.1016/j.atmosenv.2022.118946

Jendritzky, G., de Dear, R., & Havenith, G. (2012). UTCI – Why another thermal index? *International Journal of Biometeorology, 56*(3), 421–428. https://doi.org/10.1007/s00484-011-0513-7

Johnson, D. P., & Wilson, J. S. (2009). The socio-spatial dynamics of extreme urban heat events: The case of heat-related deaths in Philadelphia. *Applied Geography (Sevenoaks, England), 29*(3), 419–434. https://doi.org/10.1016/j.apgeog.2008.11.004

Junk, J., Helbig, A., & Lüers, J. (2003). Urban climate and air quality in Trier Germany. *International Journal of Biometeorology, 47*(4), 230–238. https://doi.org/10.1007/s00484-003-0162-6

Koedel, U., Dietrich, P., Herrmann, T., Liang, C., Ritter, O., Roettenbacher, J., … Schuetze, C. (2024). Enhancing citizen science impact in environmental monitoring: Targeted engagement strategies with stakeholder groups. *Frontiers in Environmental Science, 12*, 1375675. https://doi.org/10.3389/fenvs.2024.1375675

Leconte, F., Bouyer, J., & Claverie, R. (2020). Nocturnal cooling in Local Climate Zone: Statistical approach using mobile measurements. *Urban Climate, 33*, 100629. https://doi.org/10.1016/j.uclim.2020.100629

Lehnert, M., Geletič, J., Kopp, J., Brabec, M., Jurek, M., & Pánek, J. (2021b). Comparison between mental mapping and land surface temperature in two Czech cities: A new perspective on indication of locations prone to heat stress. *Building and Environment, 203*, 108090. https://doi.org/10.1016/j.buildenv.2021.108090

Lehnert, M., Savić, S., Milošević, D., Dunjić, J., & Geletič, J. (2021a). Mapping Local Climate Zones and Their Applications in European Urban Environments: A Systematic Literature Review and Future Development Trends. *ISPRS International Journal of Geo-Information, 10*(4), 260. https://doi.org/10.3390/ijgi10040260

Loglisci, N., Milelli, M., Iurato, J., Galia, T., Galizia, A., & Parodi, A. (2024). Validation of Citizen Science Meteorological Data: Can They Be Considered a Valid Help in Weather Understanding and Community Engagement? *Sensors (Basel), 24*(14), 4598. https://doi.org/10.3390/s24144598

Marquès, E., Masson, V., Naveau, P., Mestre, O., Dubreuil, V., & Richard, Y. (2022). Urban Heat Island Estimation from Crowdsensing Thermometers Embedded in Personal Cars. *Bulletin of the American Meteorological Society, 103*(4), E1098–E1113. https://doi.org/10.1175/BAMS-D-21-0174.1

Matzarakis, A., Rutz, F., & Mayer, H. (2010). Modelling radiation fluxes in simple and complex environments: Basics of the RayMan model. *International Journal of Biometeorology, 54*(2), 131–139. https://doi.org/10.1007/s00484-009-0261-0

Meier, F., Fenner, D., Grassmann, T., Otto, M., & Scherer, D. (2017). Crowdsourcing air temperature from citizen weather stations for urban climate research. *Urban Climate, 19*, 170–191. https://doi.org/10.1016/j.uclim.2017.01.006

Middel, A., Nazarian, N., Demuzere, M., & Bechtel, B. (2022). Urban Climate Informatics: An Emerging Research Field. *Frontiers in Environmental Science, 10*, 867434. https://doi.org/10.3389/fenvs.2022.867434

Moderow, U., Ziemann, A., Goldberg, V., & Sinning, H. (2023). Thermal loads in two different urban quarters – perspectives from mobile measurements and mental maps. *Meteorologische Zeitschrift (Berlin), 32*(6), 447–470. https://doi.org/10.1127/metz/2023/1175

Muse, N., Clement, A., & Mach, K. J. (2024). Daytime land surface temperature and its limits as a proxy for surface air temperature in a subtropical, seasonally wet region. *PLOS Climate, 3*(10), e0000278. https://doi.org/10.1371/journal.pclm.0000278

Nipen, T. N., Seierstad, I. A., Lussana, C., Kristiansen, J., & Hov, Ø. (2020). Adopting Citizen Observations in Operational Weather Prediction. *Bulletin of the American Meteorological Society, 101*(1), E43–E57. https://doi.org/10.1175/BAMS-D-18-0237.1

Ohashi, Y., Genchi, Y., Kondo, H., Kikegawa, Y., Yoshikado, H., & Hirano, Y. (2007). Influence of Air-Conditioning Waste Heat on Air Temperature in Tokyo during Summer: Numerical Experiments Using an Urban Canopy Model Coupled with a Building Energy Model. *Journal of Applied Meteorology and Climatology, 46*(1), 66–81. https://doi.org/10.1175/JAM2441.1

Oke, T. R. (1987). *Boundary Layer Climates* (2nd ed.). London, New York: Routledge.

Oke, Timothy R., Mills, G., Christen, A., & Voogt, J. A. (2017). *Urban climates.* Cambridge: Cambridge University Press. http://www.gbv.de/dms/tib-ub-hannover/872088057.pdf

Parlow, E., & Foken, T. (2021). Ground-based Mobile Measurement Systems. In T. Foken (Ed.), *Springer Handbook of Atmospheric Measurements* (pp. 1351–1367). Cham: Springer International Publishing; https://doi.org/10.1007/978-3-030-52171-4_50

Rink, D., & Schmidt, C. (2021). Afforestation of urban brownfields as a nature-based solution. Experiences from a project in Leipzig (Germany). *Land (Basel), 10*(9), 169–185. https://doi.org/%20 10.3390/land10090893 https://doi.org/10.3390/land10090893

Samad, A., & Vogt, U. (2020). Investigation of urban air quality by performing mobile measurements using a bicycle (MOBAIR). *Urban Climate, 33*, 100650. https://doi.org/10.1016/j.uclim.2020.100650

Schmidt, F., Schütze, C., Ködel, U., Schütze, F., Liang, C., Schäfer, D., & Dietrich, P. (2023, April 23). *Comparison of Mobile Environmental Sensors for Citizen Science Based Climate Monitoring*. EGU-12542. Vienna, Austria. https://doi.org/10.5194/egusphere-egu23-12542

Stewart, I. D., Krayenhoff, E. S., Voogt, J. A., Lachapelle, J. A., Allen, M. A., & Broadbent, A. M. (2021). Time Evolution of the Surface Urban Heat Island. *Earth's Future, 9*(10), e2021EF002178. https://doi.org/10.1029/2021EF002178

Stewart, I. D., & Oke, T. R. (2012). Local climate zones for urban temperature studies. *Bulletin of the American Meteorological Society, 93*(12), 1879–1900. https://doi.org/10.1175/BAMS-D-11-00019.1

Todorov, A., Gicheva, P., Stoykova, V., Karapetkov, S., Uzunov, H., Dechkova, S., & Zlatev, Z. (2023). Environmental Monitoring in Bus Transportation Using a Developed Measurement System. *Urban Science (Basel, Switzerland), 7*(3), 90. https://doi.org/10.3390/urbansci7030090

Tong, S., Prior, J., McGregor, G., Shi, X., & Kinney, P. (2021). Urban heat: An increasing threat to global health. *BMJ (Clinical Research Ed.), 375*(2467), n2467. https://doi.org/10.1136/bmj.n2467

Tsin, P. K., Knudby, A., Krayenhoff, E. S., Ho, H. C., Brauer, M., & Henderson, S. B. (2016). Microscale mobile monitoring of urban air temperature. *Urban Climate, 18*, 58–72. https://doi.org/10.1016/j.uclim.2016.10.001

Yang, J., Yu, W., Baklanov, A., He, B., & Ge, Q. (2025). Mainstreaming the local climate zone framework for climate-resilient cities. *Nature Communications, 16*(1), 5705. https://doi.org/10.1038/s41467-025-61394-w

Yokoyama, H., Ooka, R., & Kikumoto, H. (2018). Study of mobile measurements for detailed temperature distribution in a high-density urban area in Tokyo. *Urban Climate, 24*, 517–528. https://doi.org/10.1016/j.uclim.2017.06.006

Zhou, D., Xiao, J., Bonafoni, S., Berger, C., Deilami, K., Zhou, Y., … Sobrino, J. A. (2019). Satellite Remote Sensing of Surface Urban Heat Islands: Progress, Challenges, and Perspectives. *Remote Sensing (Basel), 11*(1), 48. https://doi.org/10.3390/rs11010048

Manuscript received: March 29, 2025
Revisions requested: June 19, 2025
Final revised version received: February 13, 2025
Manuscript accepted: March 1, 2026

Appendix

Please note that there is no agreed standard, how the accuracy and uncertainty of measurements devices by the manufacturer must be reported concerning the range to which the reported accuracy and uncertainty, respectively, is given.

Table A1. Mobile System – MeteoTracker, manufacturer information and information about measurement accuracy as indicated by the manufacturer.

Variable	Measurement device/sensor	Manufacturer	Accuracy[&]
Air temperature	TMP117	Texas Instruments	sensor +/−0.1 °C @−25…+50 °C, incl. solar radiation error: +/−0.5 °C @ speed > 10 km/h
Relative humidity	HDC3022	Texas Instruments	±0.5%
Air pressure	Bosch BMP390	Bosch	±0.05 hPa
Position and time	depends on smartphone GNSS receiver	depends on smartphone GNSS receiver	< 5m (horizontal)

[&] As noted by the respective manufacturer.

Table A2. Mobile System – SenseBox, manufacturer information and information about measurement accuracy as indicated by the manufacturer.

Variable	Measurement device/sensor	Manufacturer	Accuracy[&]
Air temperature	Bosch BME680	Bosch	−40 … 85 °C, @25 °C ± 0.5 °C
Relative humidity	Bosch BME680	Bosch	0–100%, ± 3%
Air pressure	Bosch BME680	Bosch	300–1100 hPa, ± 1 hPa
CO_2 concentration	Sensirion SCD30	Sensirion	± (30 ppm + 3% of measured value) @400–10000 ppm
Position and time	GNSS	Watterott, CAM-M8	±2.5 m (horizontal)
Particle concentration 0.3 to 10 µm[#]	Nova Fitness SDS011	Nova Fitness	Resolution up to 0.3 µg/cm³)

[&] As noted by the respective manufacturer.
[#] Particulate matter PM_{10} and $PM_{2.5}$.

Table A3. Mobile System – Backpack, manufacturer information and information about measurement accuracy as indicated by the manufacturer.

Variable	Measurement device/sensor	Manufacturer	Accuracy[&]
Air temperature	Weather Transmitter WXT 520[§]	Vaisala, Vantaa, Finnland	± 0.3 °C at 20 °C
Relative humidity	Weather Transmitter WXT 520[§]	Vaisala, Vantaa, Finnland	± 3% over 0 to 90%
Wind speed	Weather Transmitter WXT 520	Vaisala, Vantaa, Finnland	± 3% at 10 m s^{-1}
Shortwave radiation	Pyranometer SKS 1110	Skye Instruments, Llandrindod Wells, UK	± 5%
Surface temperature (downwards)	Infra-red Remote Temperature Sensor IR120[§]	Campbell Scientific, Logan, USA	± 0.2 °C at 50 °C
Position and time	GPS16X-HVS	Garmin Ltd, USA	< 3 m

[&] As noted by the respective manufacturer.
[§] Used with radiation shield.

Table A4. Stationary system – Bresser compact weather station, manufacturer information and information about measurement accuracy as indicated by the manufacturer.

Variable	Measurement device	Manufacturer	Accuracy[&]
Air temperature	Ventus weather station	Bresser	± 0.4 °C over 5.1 °C to 60 °C
Relative humidity	Ventus weather station	Bresser	± 3.5% over 21%–80%
Precipitation	Ventus weather station	Bresser	Resolution: 0.4 mm Uncertainty ± 7%
Wind speed	Ventus weather station	Bresser	Resolution: 0.1 m s^{-1} Uncertainty ± 6%

[&] As noted by the respective manufacturer.

Table A5. Stationary system – Professional climate station at open area (c.f. Fig. 4, 5) manufacturer information and information about measurement accuracy as indicated by the manufacturer.

Variable	Measurement device/sensor	Manufacturer	Accuracy[&]
Air temperature	CS215[#]	Campbell Scientific, Logan, USA	± 0.4 °C over + 5 °C to + 40 °C
Relative humidity	CS215[#]	Campbell Scientific, Logan, USA	± 4% over 0–100%
Shortwave radiation	SP-110	Apogee Instruments, Logan, USA	± 5%
Wind speed	Wind monitor 5305	Campbell Scientific, Logan, USA	± 0.2 m s^{-1} or 1% of reading
Wind direction	Wind monitor 5305	Campbell Scientific, Logan, USA	± 3%

[&] As noted by the respective manufacturer.
[#] Sensing element: Sensirion SHT75.

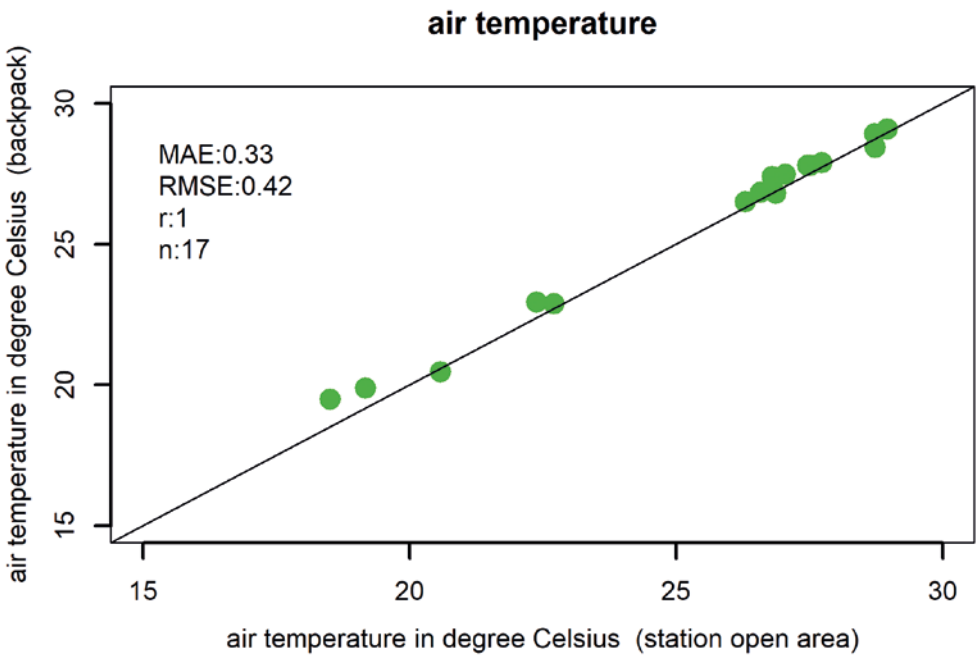

Fig. A1. Comparison of T_{air} data obtained via backpack during short stationary comparison periods to T_{air} data of climate station "open area" reference station. MAE – mean absolute error, RMSE – root mean square error, r-Pearson correlation coefficient, n – number of used data pairs. MAE and RMSE in °C.

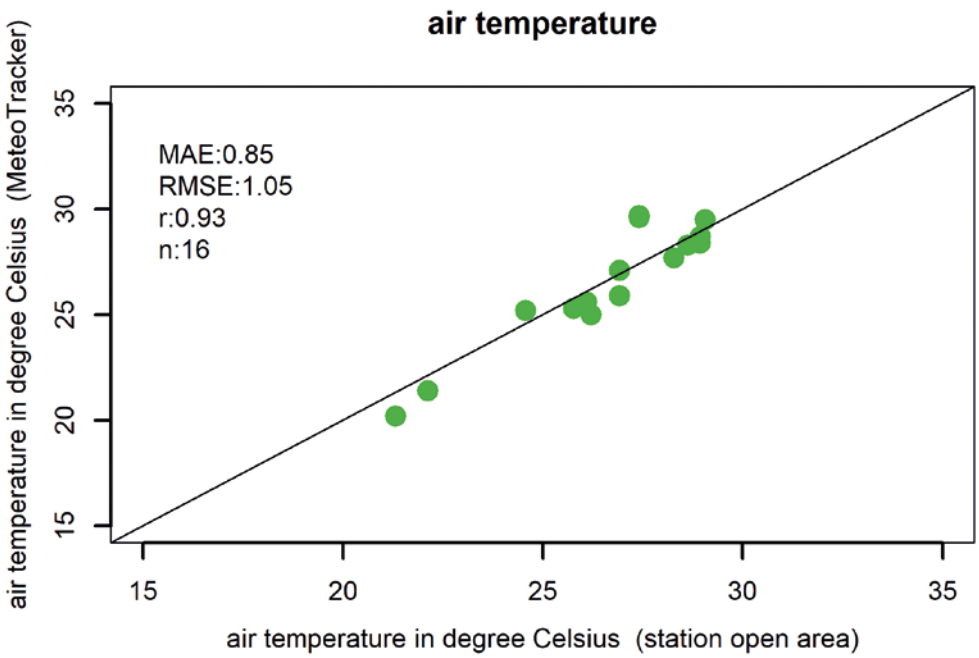

Fig. A2. Comparison of T_{air} data obtained via bicycle in combination with MeteoTracker to T_{air} data of climate station "open area" reference station. All data points recorded by MeteoTracker within a radius of 30 m of the climate station "open area" were used. MAE – mean absolute error, RMSE – root mean square error, r-Pearson correlation coefficient, n – number of used data pairs. MAE and RMSE in °C.

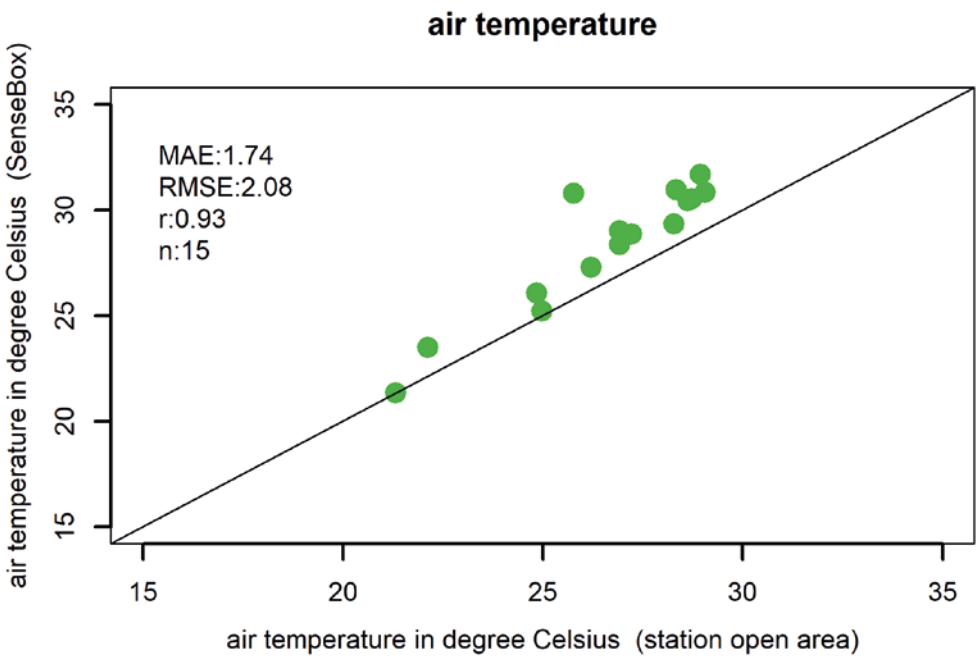

Fig. A3. Comparison of T_{air} data obtained via bicycle in combination with SenseBox to T_{air} data of climate station "open area" reference station. All data points recorded by SenseBox within a radius of 30 m of the climate station "open area" were used. MAE – mean absolute error, RMSE – root mean square error, r-Pearson correlation coefficient, n – number of used data pairs. MAE and RMSE in °C.